Continual renewal and replication of persistent *Leishmania major* parasites in concomitantly immune hosts

Michael A. Mandell[a,1] and Stephen M. Beverley[a,2]

[a]Department of Molecular Microbiology, Washington University School of Medicine, St. Louis, MO 63110

Contributed by Stephen M. Beverley, December 15, 2016 (sent for review November 22, 2016; reviewed by Arturo Casadevall and Phillip Scott)

In most natural infections or after recovery, small numbers of *Leishmania* parasites remain indefinitely in the host. Persistent parasites play a vital role in protective immunity against disease pathology upon reinfection through the process of concomitant immunity, as well as in transmission and reactivation, yet are poorly understood. A key question is whether persistent parasites undergo replication, and we devised several approaches to probe the small numbers in persistent infections. We find two populations of persistent *Leishmania major*: one rapidly replicating, similar to parasites in acute infections, and another showing little evidence of replication. Persistent *Leishmania* were not found in "safe" immunoprivileged cell types, instead residing in macrophages and DCs, ∼60% of which expressed inducible nitric oxide synthase (iNOS). Remarkably, parasites within iNOS$^+$ cells showed normal morphology and genome integrity and labeled comparably with BrdU to parasites within iNOS$^-$ cells, suggesting that these parasites may be unexpectedly resistant to NO. Nonetheless, because persistent parasite numbers remain roughly constant over time, their replication implies that ongoing destruction likewise occurs. Similar results were obtained with the attenuated *lpg2*$^-$ mutant, a convenient model that rapidly enters a persistent state without inducing pathology due to loss of the Golgi GDP mannose transporter. These data shed light on *Leishmania* persistence and concomitant immunity, suggesting a model wherein a parasite reservoir repopulates itself indefinitely, whereas some progeny are terminated in antigen-presenting cells, thereby stimulating immunity. This model may be relevant to understanding immunity to other persistent pathogen infections.

latency | quiescence | trypanosomatid protozoan parasite | vaccination | stem cell-like

As long-term infection of a host can increase a pathogen's chances of transmission, many have evolved the ability to prolong their survival within their hosts. *Leishmania*, *Mycobacterium tuberculosis*, *Toxoplasma gondii*, and latent herpesviruses can remain indefinitely within their hosts in small numbers without overt pathology. Such low-level persistent infections differ considerably from "chronic" infections, where pathogen numbers are typically much higher and often accompanied by disease symptoms (1). Unfortunately the terms persistent and/or chronic are applied inconsistently or even interchangeably across pathogens, in part reflecting the evolution of our understanding, organism-specific lexicons, and diverse mechanisms used by pathogens for long-term survival within the host (1, 2). Here we focus on persistent infections exclusively of the "low numbers" type, which are of medical importance due to their ability to reactivate to severe disease (3, 4), to serve as reservoirs for transmission, and to engender a protective response against subsequent infections, a process known as concomitant immunity (5).

Persistence is a significant but understudied aspect of the biology of parasites of the genus *Leishmania*, the causative agents of leishmaniasis. These parasites are responsible for an estimated 12 million active cases, at least 120 million asymptomatic infections, and 1.7 billion people are at risk (6–9). *Leishmania* sp. are transmitted as metacyclic-stage promastigotes to humans by the bite of an infected sand fly. In the skin, parasites are engulfed by phagocytic cells, where they differentiate into the amastigote stage and begin to replicate. Although most infections are asymptomatic, a significant fraction go on to produce ulcerating skin lesions; in both cases, parasites can metastasize to other sites and cause more severe disease such as visceral or mucocutaneous leishmaniasis (9). For *Leishmania major*, in most human cases and experimental infections of "resistant" mouse strains, the infection is eventually controlled by an adaptive Th1 immune response, in a manner requiring inducible NOS (iNOS) (10, 11). Thereafter, the number of parasites in infected tissue declines dramatically, the lesion heals, and the host becomes immune to subsequent *L. major* infection (12, 13). However, a small and steady population of parasites remains at the site of infection and in the lymph node draining that site for the rest of the host's life (14).

These persistent parasites play vital roles in *Leishmania* biology. Despite their limited numbers (∼1,000), persistent parasites can be transmitted to sand fly vectors and thus could function as a transmission reservoir (6, 15, 16). Second, they pose a substantial risk to infected people in the event of immunosuppression, as the persistent parasites can "reactivate," leading to severe disease (17). Finally, they maintain protective immunity to subsequent *Leishmania* infections through concomitant immunity, which results in amelioration of disease pathology without sterilization of either the persistent or incoming parasite (18, 19). Indeed, healed *Leishmania* infections are the gold standard in anti-*Leishmania* immunity, and to date no other vaccination approaches have proven as successful in humans (18). Importantly, treatment of persistently infected mice to achieve a sterile cure renders those mice susceptible to new infections (14, 20), suggesting that the persistent parasites are required for strong, long-lasting anti-*Leishmania* immunity.

Significance

Persistent parasites contribute to the maintenance of protective immune responses through concomitant immunity, but our understanding of how they do so has been limited by the difficulties associated with their low numbers. Our studies indicate that for *Leishmania* substantial parasite replication occurs in persistent infections, with most parasites found within activated antigen-presenting cells. Parasite replication serves to maintain the infection and likely also provides a constant source of parasite antigens for immune stimulation and the maintenance of protective immunity. Collectively, these studies suggest a framework to understand concomitant immunity that may be applicable to other persistent pathogens.

Author contributions: M.A.M. and S.M.B. designed research; M.A.M. performed research; M.A.M. and S.M.B. analyzed data; and M.A.M. and S.M.B. wrote the paper.

Reviewers: A.C., Johns Hopkins Bloomberg School of Public Health; and P.S., University of Pennsylvania.

The authors declare no conflict of interest.

[1]Present address: Department of Molecular Genetics and Microbiology, University of New Mexico Health Sciences Center, Albuquerque, NM 87131.

[2]To whom correspondence should be addressed. Email: stephen.beverley@wustl.edu.

This article contains supporting information online at www.pnas.org/lookup/suppl/doi:10.1073/pnas.1619265114/-/DCSupplemental.

The host immune response is important to simultaneously prevent reactivation and clearance of persistent parasites (21, 22). Treatment of persistently infected mice with immunosuppressive drugs, iNOS inhibitors, or the blockade of IFN-γ signaling rapidly results in increased parasite numbers and the reappearance of disease symptoms (11). In contrast, depletion of $CD4^+CD25^+$ regulatory T cells or the blockade of IL-10 signaling results in sterile cure in mice (20, 23). The mechanisms used by persistent parasites to modulate the host's immune responses or to maintain protective immunity are less well understood. Indeed recent studies have drawn attention to continuing antigenic stimulation arising from the site of infection, which is better understood from the host's than parasite's perspective (24).

The study of persistent parasites poses significant experimental challenges. Typically persistence is studied after resolution of disease in a resistant (Th1) murine model, which requires >4 mo to attain (11, 25) (Fig. S1*D*). Furthermore, the low number of persistent *Leishmania* renders their visualization, much less characterization, a daunting task (26). Here we established several methods facilitating the study of both replication and host cellular localization of the scarce persistent parasites. Our data show that persistent parasites constitute two populations, one replicating and one seemingly quiescent. Similar results were found with the *lpg2*$^-$ mutant *L. major* lacking the Golgi GDP-mannose transporter, which fails to induce disease pathology even in susceptible (Th2) mice but persists indefinitely for the life of the animal (25), where it confers strong protective immunity (14, 27). Our studies suggest a model explaining how persistent *Leishmania* maintain concomitant immunity in which a small replicating reservoir acts to maintain a perpetual infection needed for transmission, while spinning off a pool of parasites destined for immune destruction and stimulation. This model potentially applies to other persistent pathogens.

Results

Assay of *Leishmania* Replication by BrdU Incorporation in Vitro. *L. major* promastigotes were incubated with 0.1 mM BrdU for various periods, followed by fixation and staining with a rat anti-BrdU monoclonal antibody to detect incorporation (28). To detect the parasite nuclei, we chose a pool of antibodies specifically recognizing *Leishmania* histones, as these epitopes proved durable to the harsh acid fixations needed to monitor BrdU incorporation. BrdU was incorporated into both the kinetoplast (mitochondrial) DNA network and the nucleus (Fig. 1*A*), and under conditions where parasites replicated with a doubling time of ∼8 h, the percent of $BrdU^+$ cells rose steadily to 90% over 9 h (Fig. 1*B*). Longer labeling times did not lead to further increase, suggesting that this was the maximum technically achievable. Under conditions of slow growth (serum reduction), a lower fraction of $BrdU^+$ parasites was observed, arising by an increase in the length of G1 phase as in most eukaryotes (Fig. S1 *A–C*). No $BrdU^+$ cells were seen in stationary phase promastigotes following 24 h of labeling. *L. major*-infected macrophages (MΦs) grown in the presence of BrdU for 72 h resulted in 90% $BrdU^+$ labeling of the intracellular amastigote stage nuclei. These studies show that BrdU labels *Leishmania* as expected, in both parasite stages and within MΦ.

Visualizing Persistent *Leishmania* and Replication in Infected Animals in Situ. For these studies, we chose to use the classical s.c. footpad inoculation model of *L. major* infection, as this allowed us to put our findings in the context of a large body of literature addressing *Leishmania* pathogenesis, immunology, persistence, and vaccination (21). To detect the low numbers of "persistent infection parasites" (PIPs), the site of footpad infection was excised, the tissue fixed, and 10 μm-thick serial sections prepared and labeled with the anti-*Leishmania* histones for confocal microscopy. In some sections, as many as 10–100 parasites were evident, wheras others had none. Integration of parasite numbers across serial sections from a single footpad yielded numbers comparable to those typically obtained with limiting dilution assays (100–2,000), suggesting that this approach was capable of detecting most parasites.

We then combined the BrdU incorporation and in situ *Leishmania* detection protocols to visualize parasite replication in infected animals. There, *Leishmania* replicates rapidly for the first 4–6 wk after inoculation (13); we refer to parasites during this period as "acute-infection parasites" (AIPs). Bioluminescent imaging of luciferase-expressing parasites showed that AIPs replicate exponentially with a doubling time of ∼60 h and as such provided an ideal setting to optimize in vivo BrdU incorporation assays.

Because mammals rapidly clear nucleosides from circulation (29), we tested several different BrdU delivery protocols as described in *Materials and Methods*, sacrificing treated mice 24 h

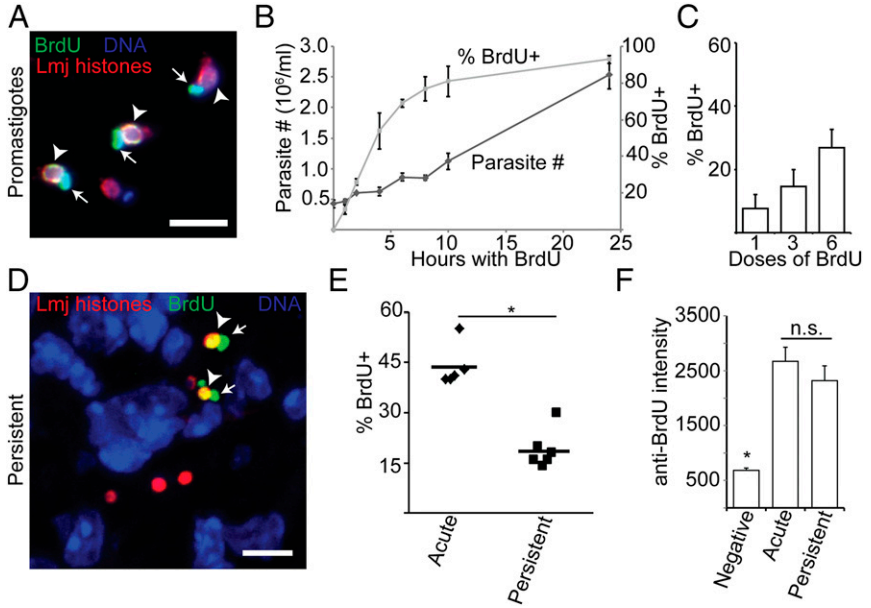

Fig. 1. BrdU incorporation assay demonstrates persistent parasite replication in situ. (*A*) Labeling of log-phase promastigotes with BrdU. (*B*) Parasite density and extent of BrdU labeling of log-phase promastigotes cultured for 24 h in the presence of BrdU. Dark-shaded diamonds, parasite number; light-shaded squares, percent $BrdU^+$. (*C*) The effect of increasing the number of BrdU doses (simultaneous local and systematic injection) on the percent $BrdU^+$ parasites during acute mouse footpad infections where parasites are growing logarithmically. $n = 3$ mice; >1,000 total parasites. (*D*) Confocal microscopic analysis of BrdU incorporation of footpad PIPs. (*E*) Comparison of the percent $BrdU^+$ intracellular parasites in AIPS versus PIPs. Data points, mean percent BrdU labeling for individual mice. Horizontal bars, mean for all mice. (*F*) Analysis of the BrdU-labeling intensity of parasite nuclei. $n = 20$ parasites per category. Graph shows mean ± SEM; $^*P < 0.05$; n.s., not significant by Student's *t* test or ANOVA. Arrowheads, BrdU-labeled nuclei; arrows, BrdU-labeled kinetoplast (mitochondrial) DNA. (Scale bar, 5 μM.)

after the start of the dosing period. Although all yielded abundant BrdU$^+$ host cell nuclei, BrdU$^+$ parasites were only detected in mice receiving multiple i.p. and s.c. footpad injections. The percentage of parasites labeled increased linearly with the number of doses, and we adopted as the maximum practicable a regimen of 6 doses given every 3 h as a "standard" (Fig. 1*C*). Assuming a 24-h labeling period and a parasite doubling time of 60 h, we calculated that 40% of AIPs should be BrdU$^+$; by the protocol above, 44 ± 6% were BrdU$^+$, in good agreement.

PIPs Replicate in Vivo. We then tested whether PIPs incorporated BrdU into their DNA. We defined the asymptomatic persistent infection phase as >1 mo following the resolution of footpad swelling at the inoculation site (typically ∼4 mo postinfection; Fig. S1*D*). In all studies, multiple experiments, mice and sections were analyzed, enabling statistical tests of distribution and significance [represented as N = E (experiments)/M (mice)/P (parasites)]. We found that 19 ± 6% of PIPs showed BrdU$^+$ nuclei (Fig. 1 *D* and *E*), about half that seen in AIPs ($P < 0.0001$). The intensity of BrdU labeling per cell was similar for AIPs or PIPs (Fig. 1*F*), implying that differences reflected the number of replicating parasites rather than the rate of BrdU incorporation. If one assumed a homogeneously replicating population, a doubling time of about 120 h could be calculated for PIPs.

For confirmation, we formulated an indirect assay based on the number of parasites per cell. This approach assumes that for PIPs, host cells are initially infected by a single parasite, as the low number renders the chance of multiple independent infections unlikely. From this we inferred that host cells containing two or more PIPs (here termed "clusters" as opposed to singletons) must have arisen exclusively through parasite replication, thereby providing an indirect metric. In contrast, for in vitro MΦ infections, which are usually performed at high multiplicities of infection (and possibly for AIPs where parasite numbers can be quite high), such an inference would not be valid. Thus, PIP cluster analysis provides an alternative perspective on replication.

In both AIPs and PIPs, we readily found clusters containing 2–20 parasites per host cell in mice that were not subjected to BrdU dosing. Consistent with the results of the BrdU incorporation assay, AIPs showed a higher proportion of parasites found in clusters, with a higher fraction containing >8 parasites than seen for PIPs (Fig. 2 *A* and *B*). Nevertheless, in persistent infections, roughly half of all infected cells contained clusters with two or more PIPs (Fig. 2*A*), and ∼80% of all PIPs were found in clusters (Fig. 2*B*). This provided independent support of PIP replication. Across all studies, singletons and clusters were interspersed, arguing against the possibility of segregation of cells harboring replicating and nonreplicating PIPs.

Persistent *Leishmania* Show Two Populations with Different Replication Rates: One "Fast," One Slow/Nonreplicating. Combining the BrdU incorporation and cluster assays allowed us to test whether PIPs replicated as a homogeneous population. We plotted the percent of parasite clusters as a function of the percent BrdU$^+$ within those clusters (Fig. 2*C*). For a homogeneous population, a distribution centered about the mean was anticipated, and indeed, this was seen with AIPs (mean BrdU$^+$ = 44 ± 6%; Fig. 2*C*). In contrast, PIPs did not show a single distribution centered around 19% labeling, instead exhibiting two peaks (Fig. 2*C*). The first peak, accounting for ∼60% of the total clusters, showed no BrdU$^+$ cells under these labeling conditions, whereas the second peak, accounting for the remaining 40% of clusters, showed a mean BrdU$^+$ of 57 ± 21%. The distribution and mean of the second population resembled that of AIP clusters (mean BrdU$^+$ of 46 ± 29%; Fig. 2*C*).

Although this suggested the existence of two populations, we were concerned that the analysis excluded singleton parasites not in clusters, about ∼20% of all PIPs. We thus reanalyzed the data by plotting the percent BrdU$^+$ cells as a function of cluster size. Assuming homogeneous parasite replication, roughly 44% of AIPs and 19% of PIPs should be BrdU$^+$, regardless of the number of parasites per host cell. AIPs very closely matched this prediction, with 40–50% BrdU$^+$ uniformly across cluster size (Fig. 2*D*). However, for PIPs only ∼12% of the parasites in host cells bearing 1–3 parasites were BrdU$^+$, whereas ∼46% of the parasites within clusters containing four or more parasites were BrdU$^+$ (Fig. 2*D*), a value very close to the maximum obtainable by these labeling conditions (Fig. 1).

By integrating the data shown in Fig. 2 *B–D* and correcting for BrdU labeling efficiency, we conclude that there are two populations in persistent *Leishmania* infections: one comprising about 61% of the total cells, whose replication properties resemble those of AIPs (replicating with a doubling time of ∼60 h; Fig. 1). In contrast, a second population comprises about 39% of the cells, which under the conditions used fail to incorporate BrdU significantly. This second population is much less abundant in AIPs (Fig. 2*C*; 0% BrdU$^+$ population). Although one could interpret the "BrdU null" population as evidence of arrested or nonreplicating PIPs, we cannot exclude the possibility that their replication is just very slow, beyond the limits of our in vivo BrdU labeling protocol.

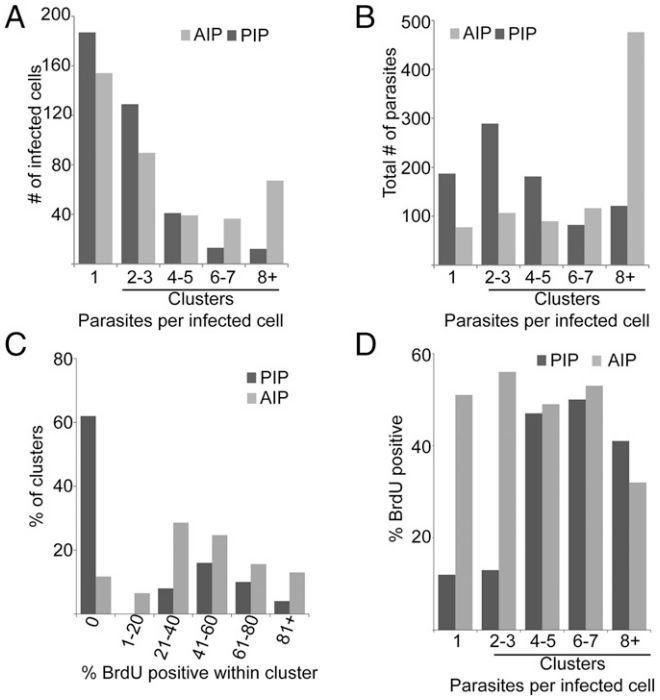

Fig. 2. Parasite cluster analysis indicates two populations of persistent parasites: actively replicating and quiescent. (*A*) Frequency of infected cells plotted as a function of the number of intracellular parasites per cell for both AIPs and PIPs, respectively. Dark bars, persistent; light bars, acute. Clusters are defined as host cells containing two or more parasites. (*B*) Distribution of parasites as a function of the number of parasites per infected cell for both AIPs and PIPs. For *A* and *B*, n = 386 infected cells, 888 parasites, from 8 infected mice (PIPs) and 380 infected cells, 865 parasites, 3 mice (AIPs). Tissue sections analyzed for *A* and *B* were obtained from mice that were not treated with BrdU. (*C*) Distribution of clusters as a function of the percent BrdU$^+$ parasites within that cluster. For PIPs, n = 127 infected cells, 755 parasites, 5 mice; for AIPs, n = 176 infected cells, 976 parasites, 5 mice. (*D*) Percent of BrdU$^+$ parasites within individual clusters plotted as a function of cluster size. For PIPs, n = 167 infected cells, 237 parasites, 6 mice; for AIPs, n = 176 infected cells, 976 parasites, 5 mice.

PIPs Predominantly Reside in MΦs and DCs. We next determined the localization of PIPs within different host cell types. Sections were taken as before and labeled with anti-*Leishmania* histone antisera and anti-host cell type-specific markers for subsequent visualization by confocal microscopy. This allowed us to confirm that parasites were actually "within" the host cells visualized across all focal planes. Three cell types have been proposed as hosts for PIPs: reticular fibroblasts (RFs), MΦs, and DCs (26, 30). Here, we defined RFs as ER-TR7$^+$, DCs as CD11c$^+$ (F4/80$^+$ or F4/80$^-$), and MΦ as F4/80$^+$, CD11c$^-$.

At the footpad site of inoculation, only 2 ± 3% of PIPs resided within ER-TR7$^+$ RFs (Fig. 3 *A* and *B* and Table 1), despite the presence of uninfected cells in all fields. In contrast, 79 ± 12% were found within F4/80$^+$ cells (MΦ + DC) and 13 ± 7% were within CD11c$^+$ DCs (Fig. 3 *A* and *B* and Table 1). By dual-staining footpad sections (Fig. 3 *A* and *C*), we found that 78 ± 9% of PIPs were within F4/80$^+$CD11c$^-$ MΦ, and 16 ± 6% were within F4/80$^+$CD11c$^+$ DCs (Table 1). Virtually all PIPs were resident within MΦ, DCs, or RFs (Fig. 3*C*), suggesting that all PIP-harboring host cell types had been found.

A prior study reported that 43% of PIPs resided in ER-TR7+ cells in the draining lymph node (DLN) (26). When we analyzed PIPs in DLN, the number of infected ER-TR7$^+$ RFs was somewhat greater (10 ± 7%), but as before most cells were F4/80$^+$ (87 ± 12%; Fig. 3 *A* and *B* and Table S1). Unlike the footpad, where most persistent parasites resided in MΦ, in the DLN most parasites were in CDC11c$^+$ DCs (61 ± 19%; Fig. 3 *A* and *B* and Table S1). This was confirmed by dual staining, with 30 ± 18% within F4/80$^+$CD11c$^-$ MΦs and 61 ± 19% within F4/80$^+$CD11c$^+$ DCs (Fig. 3 *A* and *C* and Table S1). Again, the data showed that virtually all PIPs could be assigned to MΦs, DCs, or RFs. Thus, although we did not find high levels of PIPs within RFs in either site, there was a shift from host MΦs in the footpad to DCs in the DLN.

"Cluster" Analysis Suggests Intracellular Replication in both MΦs and DCs in Persistent Infections. Because the harsh treatments needed to visualize BrdU incorporation destroy most cell type-specific epitopes, we used cluster analysis to assess in which host cell type parasite replication takes place. These studies showed that 73 ± 11% of clusters occurred within F4/80$^+$ cells (MΦ + DC; n = 3E/8M/168 clusters), whereas 17 ± 10% were within CD11c$^+$ DCs (n = 3E/8M/124 clusters). These values are similar to that seen with individual parasites (79 ± 12% and 13 ± 7%, respectively) (Table 1). We also plotted the percent of CD11c$^+$-infected cells as function of the number of parasites per cell to determine if DCs preferentially harbor the "static" subpopulation, which tends to be within host cells containing <3 parasites, but did not see any obvious correlation. Together, these data suggest that PIP replication occurs similarly in both MΦs and DCs.

F4/80$^+$ MΦ-Bearing PIPs Do Not Express an Alternative Activation Marker or Gr-1 (Ly6C). Alternatively activated (M2) macrophages MΦ might provide a more hospitable environment for PIPs, and we tested this by reactivity with the diagnostic markers RELMα and CD206 (31). As before, PIPs were within F4/80$^+$ cells (96 ± 2%), none of which expressed RELMα (Fig. S2*A*). F4/80$^+$ RELMα$^+$ cells were seen elsewhere in the sections (Fig. S2*A*, *Inset*), and 70–80% cells were RELMα$^+$ following IL-4 and IL-13 treatment of peritoneal MΦ (PEM) (Fig. S2*B*). Similar results were obtained with CD206 (Fig. S2*C*). During the resolution phase of acute infections, many *Leishmania* parasites are found in inflammatory Gr-1$^+$ cells (32, 33), which we confirmed for AIPs (71%; Fig. S2*D*). However, in PIPs this number drops to only 7%

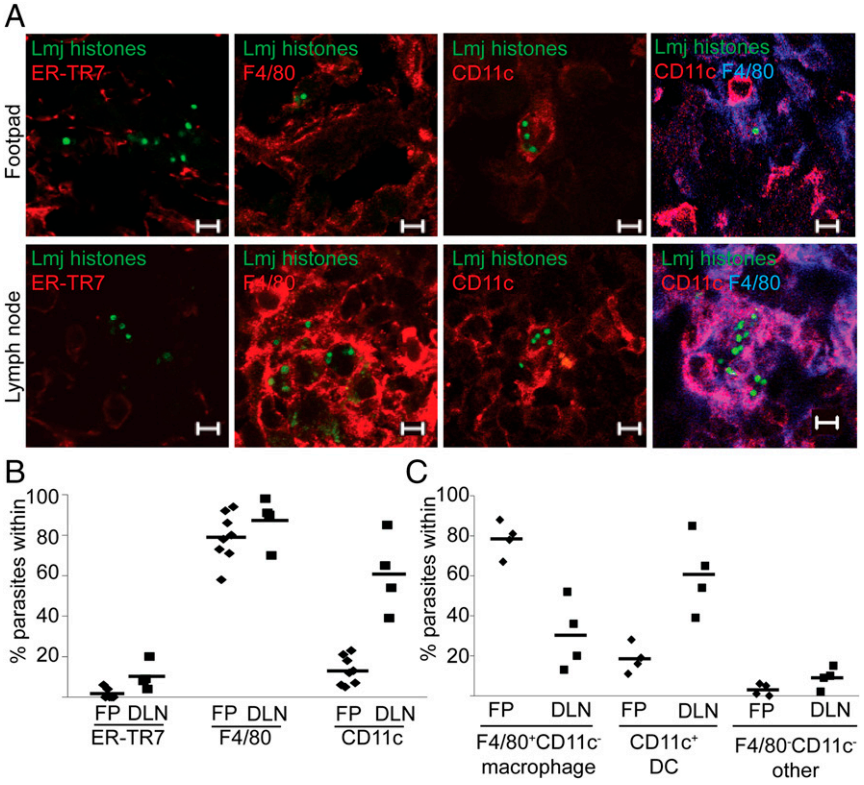

Fig. 3. PIPs are predominantly found within MΦs and DCs in footpads (inoculation site) and in DLNs. (*A*) Representative confocal micrographs of the association between PIP nuclei (green) and indicated host cell markers in footpad (FP, *Top*) and DLN (*Bottom*) tissue. (Scale bar, 5 μM.) (*B* and *C*) Quantitation of images from *A*. Data points, mean association between parasites and markers in a mouse; horizontal bars, mean for all mice.

Table 1. Quantitative immunolabeling of *L. major* PIPs at the footpad inoculation site

Labeling parameter	Percent cells	*N*, experiments (E)/mice (M)/parasites (P), in total
ER-TR7$^+$	2 ± 3	3E/6M/528P
F4/80$^+$	79 ± 12	3E/8M/983P
CD11c$^+$	13 ± 7	3E/8M/1074P
F4/80$^+$ CD11c$^-$	78 ± 9	
F4/80$^+$ CD11c$^+$	16 ± 6	2E/4M/266P
F4/80$^-$ CD11c$^+$	3 ± 3	
F4/80$^-$ CD11c$^-$	3 ± 3	
iNOS$^+$	59 ± 15	3E/8M/2535P
F4/80$^+$ iNOS$^+$	42 ± 14	3E/8M/983P
CD11c$^+$ iNOS$^+$	10 ± 6	3E/8M/1074P
RELMα$^+$	0 ± 0	2E/3M/284P
CD206$^+$	0 ± 0	2E/3M/218P
Arg1$^+$, within	3 ± 3	
Arg1, adjacent	12 ± 11	3E/5M/317P
Arg1, within + adjacent	15 ± 14	
Arg2$^+$	0 ± 0	2E/2M/175P

(Fig. S2*D*). In combination with the prior results, the majority of PIPs appear to reside within tissue MΦ.

Most PIPs Are Found Within iNOS$^+$ MΦs and DCs and Show Unexpectedly Normal Morphology, Genome Integrity, and Replication. The number of parasites in persistent *Leishmania* infections remains relatively steady for extended periods of time (14, 25), implying that PIP replication must be balanced in some manner by destruction. A likely executioner is nitric oxide (NO), generated from L-arginine via iNOS, given its role in the control of *L. major* in vivo (10, 11). Thus, we asked whether some fraction of persistent parasites was found within iNOS$^+$ host cells.

In the footpad, 59 ± 15% of PIPs were found within iNOS$^+$ cells (Table 1), whereas in the DLN 80 ± 19% percent of PIPs were within iNOS$^+$ cells (Table S1), in agreement with previous reports (34). For footpad PIPs, we confirmed the iNOS$^+$ cells were MΦs and/or DCs; 10 ± 6% of PIPs were found within CD11c$^+$/iNOS$^+$ cells (Fig. 4*A* and Table 1), whereas 42 ± 14% were found within F4/80$^+$iNOS$^+$cells, most of which are MΦs (Fig. 4*B* and Table 1).

We asked whether PIPs residing in iNOS$^+$ cells showed evidence of immune attack. To assess morphology, we used GFP-expressing parasites; for these, PIPs within iNOS$^+$ host cells were morphologically normal and indistinguishable from PIPs in iNOS$^-$ host cells (Fig. 4*C*).

Parasite genome integrity was assessed by the TUNEL assay (35). PIPs visualized in iNOS$^+$ cells showed no TUNEL$^+$ nuclei, but 26 ± 15% of PIPs showed TUNEL$^+$ kinetoplast (mitochondrial) DNA (Fig. 4*D*). This is expected in healthy cells as kinetoplast replication involves the transient formation of double-stranded breaks (36).

The "healthy" TUNEL$^+$ kinetoplast/TUNEL$^-$ nucleus pattern suggested that PIPs replicated within iNOS$^+$ cells. We tested this idea using the BrdU incorporation assay, as the iNOS antigen proved resistant to the treatments required for BrdU immunolabeling. In these experiments, 82 ± 10% of total parasites were within iNOS$^+$ cells, slightly higher than what we had observed previously. Simultaneous labeling for *Leishmania* histones and iNOS and BrdU incorporation showed that a very similar percentage of the BrdU$^+$ parasites (85 ± 15%; n = 2E/3M/254P) were within iNOS$^+$ cells. This suggests that PIPs do not preferentially replicate within iNOS-negative cells. This was verified by PIP cluster analysis, where 61 ± 9% occurred within iNOS$^+$ cells

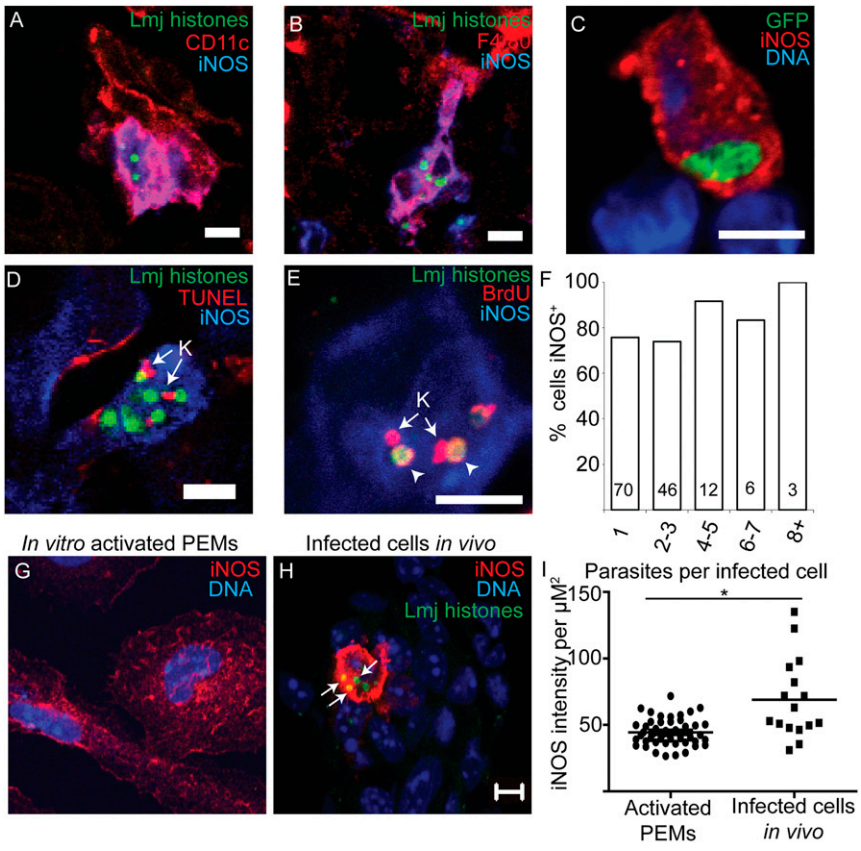

Fig. 4. PIPs are morphologically intact and replicate within iNOS-expressing cells. (*A* and *B*) Representative images of parasite nuclei (green) within iNOS-positive CD11c$^+$ (*A*) or F4/80$^+$ cells (*B*) in persistently infected footpad tissue. (*C*) GFP-expressing *L. major* (green) within iNOS-positive cells in persistently infected tissue shows expected morphology for intracellular parasites. (*D*) TUNEL labeling of PIPs within iNOS-expressing cells. K (arrow), kinetoplast showing TUNEL$^+$. No TUNEL labeling of parasite nuclei was observed. n = 2E/3M/80P. (*E*) BrdU labeling of PIPs within iNOS-expressing cells. K, kinetoplast showing BrdU-labeling. Arrowheads, BrdU$^+$nuclei. (*F*) Percent of clusters within iNOS$^+$ cells plotted as a function of the number of intracellular parasites per cell. Numbers within the bars are the number of cells visualized. (Scale bar, 5 μM.) (*G*) Representative image of starch elicited PEMs that were cultured in the presence of IFN-γ and LPS for 24 h and then stained to detect parasite histones (green), iNOS (red), and nuclei (blue). (*H*) Representative image of an infected cell in footpad tissue stained and imaged identically to the cells in *G*. Arrows, PIP nuclei within iNOS$^+$ cells. Images of activated MΦs in vitro or iNOS-expressing infected cells from footpad tissue were captured by confocal microscopy using identical settings. (Scale bar, 5 μm.) (*I*) Comparison of average red (iNOS) fluorescence intensity per μm^2 within in vitro-activated PEMs or iNOS-expressing infected cells from footpad tissue. Each data point represents one cell. Black horizontal bars represent mean for all cells. *P < 0.05, Student's t test.

(n = 3E/8M/329 clusters). A similar percentage was seen across all cluster sizes, suggesting that neither the replicating nor nonreplicating PIPs were preferentially associated with iNOS (Fig. 4*F*). This established that PIPs replicate comparably in both iNOS$^+$ and iNOS$^-$ host cells.

Interestingly, about half of the uninfected F4/80$^+$ cells adjacent to PIP-infected host cells also were iNOS$^+$ (50 ± 15%; n = 3 mice/11 fields/343 cells). In contrast, more distant cells were rarely iNOS$^+$. These data show that "bystander" cell activation occurs during persistent infections, as has also been observed in acute infections (37), and raise the possibility that once released, PIPs may enter into either iNOS$^+$ or iNOS$^-$ cells.

Evidence That Multiple Inoculations of BrdU Do Not Perturb PIP Replication or iNOS Expression. Multiple injections were required in the vicinity of the parasite infection site to obtain sufficient BrdU labeling of both AIPs and PIPs (Fig. 1*C*). This prompted us to ask whether this necessary experimental perturbation could cause induction and/or inhibition of PIP replication in some manner. We compared PIP replication in BrdU-treated mice with that of untreated mice by the "cluster analysis" method. PIP clustering from BrdU-treated mice was determined by imaging tissue sections stained to detect parasite histones and iNOS, whereas the data from control mice were determined as part of the analysis of the host cell types containing persistent *Leishmania* (Fig. 3). This comparison showed that the distribution of parasite clusters was indistinguishable in experiments in which BrdU labeling was performed from those where it was not (Fig. S3; $P > 0.6$ by two-way ANOVA). We also tested whether the BrdU administration protocol affected the level of iNOS expression in infected host cells. In tissue from BrdU-treated mice, 65 ± 21% of the parasites were within iNOS$^+$ cells, not significantly different than that seen in mice that had not been subjected to BrdU treatment (59 ± 15%; $P = 0.38$). Thus, neither the multiple inoculations nor the presence of BrdU appear to result in detectable perturbation of either iNOS expression or PIP replication in vivo.

How Do PIPs Survive Within iNOS Host Cells? We considered several models to account for the unexpected abundance, survival, and morphological normality of PIPs within iNOS$^+$ host cells. Methods for direct in situ detection of NO are not well developed nor readily applied to the low levels of tissue PIPs seen; thus, our attempts to establish NO production by PIP-infected iNOS$^+$ cells were unsuccessful (on both control and test samples). Nevertheless, we found that iNOS expression in PIP-infected cells was somewhat higher than in IFN-γ/LPS-activated PEMs (1.6-fold; Fig. 4 *G–I*; $P < 0.001$) that kill *L. major* promastigotes in an iNOS-dependent manner (38), indicating that PIP survival is not explained by reduced iNOS expression. Next, we asked whether host or parasite arginase was up-regulated, which could deprive cells of the essential substrate for NO synthesis. PIP-bearing host cells were scored for expression of iNOS and arginase 1 (cytosolic) or 2 (mitochondrial) (39), as were adjacent cells in physical contact with the parasite-infected cell, as these could deplete arginine in their immediate vicinity (40). Although 83 ± 14% of PIPs were within iNOS$^+$ cells in these experiments, only 3 ± 3% were within iNOS$^+$Arg1$^+$ cells, and only 12 ± 11% of PIPs in iNOS$^+$ were adjacent to Arg1$^+$ cells (Fig. S4*A* and Table 1). This result is in keeping with our finding that PIPs were not found within MΦs showing hallmarks of alternative activation. We did not detect any spatial association between PIPs and Arg2$^+$ host cells (Table 1), which could be seen distantly from parasites (>75 μm; Fig. S4*B*). Lastly, although *L. major* also express arginase, promastigotes do not express enough to affect NO production by activated MΦs in vitro (41). Our studies revealed that arginase levels were reduced twofold in PIPs relative to cultured promastigotes (Fig. S4 *C–E*; $P = 10^{-6}$). Thus, up-regulation of arginase does not contribute to PIP survival in iNOS$^+$ cells.

PIPs could be intrinsically resistant to NO, as there is increasing evidence that NO may act against amastigotes by mechanisms other than toxicity (42–44). In the absence of an in vitro PIP model, as a surrogate we compared the relative NO tolerance of amastigotes to purified infectious metacyclic promastigotes following MΦ infection and induction of NO by IFN-γ/LPS activation (45). Activation increased NO levels by 20–30-fold (Fig. 5*A*) and reduced the number of parasites remaining in infected cells by 90% ($P < 0.05$; Fig. 5*B*) by 24 h after stimulation. Stimulated MΦs died by 48 h after IFN-γ/LPS activation, precluding assessment at later time points. Inclusion of the specific iNOS inhibitor L-NIL restored metacyclic survival, establishing iNOS dependency (Fig. 5 *A* and *B*). Amastigote tests were performed by first infecting with metacyclics and allowing parasites to differentiate into amastigotes before activation. Whereas prior promastigote infection interferes with MΦ activation and NO production (46), we found this effect was only transient, with infected host cells fully able to express iNOS and generate NO 3 d following infection (Fig. S5). Despite the induction of high levels of NO comparable to that seen in metacyclic infections, many more amastigotes (64 ± 2%) now survived, which was restored to 85% by NIL treatment (Fig. 5 *A* and *B*). These data suggest that amastigotes are more tolerant of NO than promastigotes (64% vs. 9% survival; $P < 0.001$), a finding which could extrapolate to both AIPs and PIPs in vivo.

Attenuated *lpg2*$^-$ *L. major* Closely Resembles WT in Persistent Infections. *L. major* lacking the Golgi GDP-mannose transporter required for lipophosphoglycan synthesis encoded by *LPG2* (*lpg2*$^-$) persist in the absence of pathology in mouse infections and vaccinate mice effectively (25). *lpg2*$^-$ may be a more amenable model for the study of persistence, as it immediately attains numbers comparable to WT PIPs within a few days after inoculation (25). Thus, we determined the cell types infected by *lpg2*$^-$ in footpad tissue in BL6 mice and whether these parasites replicate. Experiments were performed 1 mo after infection to exclude potential nonspecific inflammatory responses induced immediately after infection.

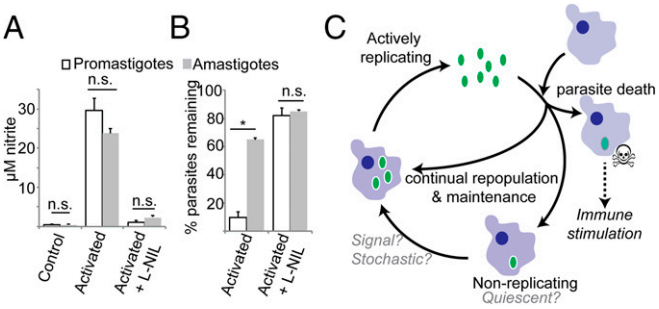

Fig. 5. Intracellular amastigotes are unexpectedly resistant to NO killing. PEMs were either pretreated with IFN-γ and LPS 2 h before infection with metacyclic promastigote-stage parasites (promastigotes, open bars) or were first infected with metacyclic-stage parasites and then treated with IFN-γ and LPS 72 h after infection (amastigotes, gray bars). NO production (*A*) and the number of parasites per infected MΦ were determined by microscopy 24 h after IFN γ/LPS treatment. (*B*) The percent of parasites remaining relative to that seen in untreated MΦs at the same time point. Graphs show mean ± SEM; *$P < 0.05$; n.s., not significant by Student's t test. (*C*) Model of *Leishmania* persistence and concomitant immunity. Persistent *Leishmania* (green oval) are found in two populations. The first population replicates similarly to parasites in acute infections, whereas the other population replicates very slowly and may be quiescent. Although some of the progeny of the replicating parasites repopulate the replicating or quiescent parasite pools, many progeny parasites are killed. Parasite replication serves to maintain persistence while simultaneously providing a continuous supply of *Leishmania* antigen, resulting in life-long immune stimulation.

For most properties, *lpg2*$^-$ PIPs were similar to WT, including the extent of BrdU labeling and residence primarily within tissue MΦ and DCs, as assessed by labeling for F4/80, CDC11c, iNOS, RELMα, ER-TR7, and Arg2 (Table S2). These data suggest that *lpg2*$^-$ parasites provide an excellent model for long-term persistent *L. major*.

For three markers, modest differences were seen. First, transiently elevated levels of *lpg2*$^-$ PIPs were found in CD206+ cells after 1 mo (50 ± 26%; $P < 0.05$), which declined to the WT levels (4 ± 5%) after 5 mo (Fig. S6*A* and Table S1). Second, the frequency of *lpg2*$^-$ PIPs within CD11c$^+$ cells was elevated threefold relative to WT (46 ± 29%; Fig. S6*B*; $P < 0.006$; Table S1), and their association with Arg1 elevated fivefold (Fig. S6*C* and Table S1; $P = 0.002$; 37% within and 35% adjacent). Unlike CD206 localization, these differences did not return to WT after 5 mo (Fig. S6*C*). Whether these differences contribute to the ability of *lpg2*$^-$ to vaccinate (14, 27) will be addressed in future studies.

Discussion

Persistent Infection *Leishmania* Comprise Two Populations, One Fast Replicating and a Second Showing Little if any Replication. Because the number of persistent parasites remains steady over long periods of time in *L. major* following resolution of infection pathology, an unanswered question was whether these parasites lay in a quiescent, nonreplicating state. As in other pathogens, this has profound consequences to strategies used for MΦ survival and immune evasion. Here, we demonstrate that a major fraction of PIPs replicate comparably to AIPs, using three independent approaches. First, we formulated a parasite cluster assay, reasoning that host cells bearing more than one parasite arose via parasite replication rather than multiple infections. Such clusters were identified both in footpads and DLNs (Figs. 2 and 3 *A* and *B*), indirectly suggesting PIP replication at both sites. Second, by the TUNEL assay, we detected significant levels of kinetoplast (mitochondrial) DNA replication (Fig. 4). The definitive evidence for PIP replication came from BrdU incorporation, which revealed that a substantial percentage of PIPs were BrdU+ (Fig. 1). Thus, many PIPs undergo active replication.

As the fraction of BrdU+ PIPs was about half of that seen with AIPs (19 vs. 44%; Fig. 1*E*), we asked whether this arose from differences in overall replication rate or population heterogeneity. This was tested by quantitative analysis of the distribution of BrdU+ parasites versus cluster size (Fig. 2), postulating that clusters comprising multiple parasites/host cells were a sign of parasite replication. As expected, AIPs showed the distribution expected for a homogeneously replicating population, with similar BrdU labeling across all cluster sizes. In contrast, PIPs showed two populations—one of whose properties closely resembled that of AIPs and a second of small clusters—showing no BrdU incorporation by our labeling protocol; indeed, BrdU$^-$ "singletons" were most numerous (Fig. 2*C*). Although we cannot rule out that these parasites are very slowly replicating by the methods available, we estimate that about 39% of PIPs fall into this nonreplicating class.

Do Slowly/Nonreplicating PIPs Enter a Quiescent Metabolic State? Potentially, slowly/nonreplicating BrdU$^-$ PIPs have entered a different metabolic state than the actively replicating BrdU$^+$ PIPs. Indeed, recently it was shown that progressive chronic infections of *Leishmania mexicana* were comprised of slowly replicating parasite populations that were metabolically relatively quiescent (47). However, the methods used there for the study of large numbers of parasites in chronic infections are not extensible to the low levels of PIPs seen in *L. major* nor for mixed populations showing widely varying replication rates. Thus, other approaches will be required to explore the metabolic status of the slowly/nonreplicating *L. major* PIPs. NO synthesis may act to dampen parasite metabolism in AIPs (42, 43), and this likely occurs with PIPs as well. The quiescent forms of many pathogens show differences in gene expression from actively replicating forms (48, 49). Similar knowledge would aid our understanding of *Leishmania* persistence considerably.

Is There a "Safe" Cell for *Leishmania* in Persistent Infections? Resolution of *L. major* infections following infection of resistant mouse strains is known to be dependent on the production of NO via iNOS (34). To account for the emergence of PIPs, investigators have posited the existence "safe cells" free from immune attack (26, 50). Although RFs or alternatively activated MΦs were attractive candidates to harbor persistent organisms (26, 31), few PIPs could be found within them (Table 1).

Instead, virtually all PIPs were found in cells often considered "unsafe"—namely, MΦs or DCs—especially given that most of these expressed iNOS at levels comparable to that seen in classically activated MΦs (Table 1 and Fig. 4). PIPs in iNOS$^+$ host cells appeared strikingly normal: their replication profiles resembled those parasites within iNOS$^-$ host cells, as did their morphology (amastigote-like) and genome integrity.

This raised the question as to how PIPs could withstand the presumptive action of iNOS through NO production. Using MΦ infections in vitro as a surrogate for AIPs and PIPs, we found the survival of amastigotes to greatly exceed that of infectious metacyclics (Fig. 5). Correspondingly, several studies suggest that the action of NO against amastigotes may be based more on metabolic inhibition rather than killing (42, 43), arising from a tissue-wide "collective" effect (44). This would likely be less effective at low PIP densities seen in persistent infections. We saw no evidence of attenuation of NO production by substrate competition with host or parasite arginase nor of other previously described mechanisms of modulating or rendering iNOS activity ineffective (51, 52). An interesting question concerns the contribution of reactive oxidant species, as infections of *phox*– mice lacking the major phagocyte oxidase (gp91/phox) often yield uncontrolled infections, albeit less reproducibly and progressing much less rapidly than seen in infections of iNOS knockout mice (53, 54). However, the lack of gp91 oxidase-specific inhibitors has precluded tests of its role specifically in PIP control, as shown elegantly using specific inhibitors of iNOS (11).

The most plausible scenario accounting for current data is that PIP-bearing host cells synthesize NO via iNOS expression, to which PIPs are largely but perhaps not entirely resistant. We have as yet not seen evidence of PIPs destruction microscopically, although the rapidity by which killed parasites disappear (Fig. 5*B*) (35) suggests the anticipated "corpses" might be difficult to visualize in vivo.

***lpg2*$^-$ as a Model for Persistence.** Previous work has shown that although attenuated in acute infections and unable to induce pathology, the *L. major lpg2*$^-$ mutant can persist indefinitely in numbers comparable to WT persistent parasites (25) and can vaccinate susceptible (BALB/c) mice against virulent challenge (27). Because *lpg2*$^-$ effectively enters the "persistent" phase very quickly, we proposed that it could provide a more convenient model than the study of healed persistent WT infections, which require >5 mo to establish. This prediction is now supported by our finding that after only 1 mo *lpg2*$^-$ was indistinguishable from WT PIPs in most respects, including the extent of replication and residence primarily with MΦs and DCs, the majority of which were iNOS$^+$ (Table S1). Preliminary data also suggest that *lpg2*$^-$ recruits Foxp3$^+$ cells to the site of infection in BALB/c mice, a phenomenon reported for WT PIPs (20). Modest differences were seen with a few markers (CD206 transiently, Arg1, and CD11c; Fig. S5), which may reflect the absence of phosphoglycans or other metabolites in the *lpg2*$^-$ and could contribute to the immune response and ability to vaccinate (25, 27, 55). Overall,

these data support the continued use of *lpg2*– parasites as a model of *Leishmania* persistence and vaccination.

A Model of *Leishmania* Persistence and Concomitant Immunity. Our data show that PIPs comprise two populations of cells: one replicating similarly to logarithmically growing acute phase parasites (~60 h doubling time), and a second population replicating much less rapidly, and possibly not at all. However, despite replication of the fast population, estimated to comprise ~61% of the total cells, PIP numbers do not increase over time, implying that parasite replication is matched by killing. Thus, the offspring of replicating parasites have three potential fates: They may continue active replication, enter a nonreplicating state, or be destroyed (Fig. 5*C*). Similarly, nonreplicating parasites may remain dormant or at some frequency resume replication. How these eventual fates are decided is not yet known. This could be under cellular regulation and control, transitioning between an active, replicating state and a potentially quiescent nonreplicating state, as seen in other pathogens exhibiting dormancy or latency. Alternatively, the fact that both replicating and quiescent PIPs reside in similarly unsafe host cells suggests a stochastic model, where forces favoring parasite persistence (such as IL-10/Treg-dependent suppression) are balanced against those favoring destruction (56), leading to maintenance of roughly constant numbers. In reality, knowledge is limited concerning how "steady" persistent *Leishmania* numbers actually are, with current data being mostly of low temporal resolution and high granularity. Thus, a model wherein parasite numbers oscillate within some range over time in response to these competing forces could be invoked. Strong perburbations of the host's response could further push persistent parasites along either path, resulting in reactivation or sterile cure (11, 20).

The ongoing replication and destruction of persistent *Leishmania* provides an attractive model for concomitant immunity and a compelling rationale for the superiority of "live" vaccination strategies in *Leishmania*. Killed parasites arising as a byproduct of parasite replication would be a good source of antigen for maintaining a robust anti-*Leishmania* response at the very site of initial infection (24). Provision of "dead antigen" in situ would also overcome the ability of live parasites to inhibit antigen presentation (57–59). Thus, from the host's perspective, persistent parasites serve as a continually self-renewing stimulatory vaccine. In some respects, the model proposed for PIP replication and "termination" is reminiscent of a stem cell cycle (Fig. S7) with some of the progeny of replicating PIPs serving as a continually self-renewing "stem" maintaining parasite persistence, whereas the remainder meet their terminal fate in antigen-presenting cells.

The continually replicating immunogen model may provide a new perspective with which to view the immune response to other persistent pathogens. For most of these, the experimental focus has been on the role of the immune system in pathogen suppression and containment, leaving the question of whether this contributes to resistance to subsequent challenges as seen with *L. major*. Following resolution of primary infections and the generation of persistent (*Toxoplasma* bradyzoites) or latent states (herpesviruses), sporadic subclinical reactivations often occur, leading to the synthesis of antigen and immune stimulation (60, 61). There is evidence that both of these persistent/latent infections may confer protection to rechallenge (62–64). Similarly, there is evidence that latent *M. tuberculosis* may undergo limited replication (65) and that latent, asymptomatic infections are associated with significant resistance to active disease (66). Future work will be needed to establish whether a continually renewing "stem-like" immunogen model is relevant to these or other persistent pathogens.

Materials and Methods

Parasite Strains and Culture. *L. major* strain LV39c5 (Rho/SU/59/P) and its derivative *lpg2*$^-$ (Δ*lpg2::HYG*/Δ*lpg2::HYG*) (25) were used in all experiments, except for the promastigote experiments show in Fig. 1 and Fig. S1, which used *L. major* strain Friedlin V1 (MHOM/IL/80/Friedlin). Parasites were grown at 26 °C in M199 medium (US Biologicals) supplemented with 40 mM 4-(2-hydroxyethyl)-1-piperazine-ethanesulfonic acid (Hepes) pH 7.4, 50 μM adenosine, 1 μg·mL^{-1} biotin, 5 μg·mL^{-1} hemin, 2 μg·mL^{-1} biopterin, and 10% (vol/vol) heat-inactivated FCS (67). "Slow-growing" promastigote cultures were grown in RPMI 1640 + L-glutamine (Invitrogen) supplemented with 37 mM Hepes pH 7.4, 47 μM adenosine, 0.93 μg·mL^{-1} biotin, 4.7 μg·mL^{-1} hemin, 1.9 μg·mL^{-1} biopterin, and 0.9% (vol/vol) heat-inactivated FCS (68). The WT LV39c5 parasites used here expressed GFP from the ribosomal locus (*SSU::IR1SAT-GFP*) and were generated by transfecting SwaI-cut plasmid B3538 into WT LV39c5 as described (67) and selecting for resistance to 100 μM nourseothricin and bright green fluorescence. The clone used in this study exhibited virulence similar to WT in BALB/c mice. Null mutants of the parasite arginase gene (Δ*arg::HYG*/Δ*arg::PAC*) (69) were cultured in the above media supplemented with 50 mM putrescine. Infective metacyclic-stage parasites were recovered using the density gradient centrifugation method (70). Propidium iodide staining of promastigotes was performed as described (71).

Antibodies Used. *L. major* nuclei were detected with a pool of rabbit antibodies raised against *L. major* histones H2A, $H2A_{variant}$, H2B, H3, and H4 (pooled at a ratio of 3:2:3:3:1 by titer, kindly provided by I. L. K. Wong, Washington University School of Medicine, St. Louis) (72). For some experiments, this pool was used at a dilution of 1:750. For others, this pool of antibodies was directly conjugated to Alexafluor488 according to the manufacturer's protocol (Invitrogen) and used at a final concentration of 0.15 mg·mL^{-1}. GFP was detected with a chicken anti-GFP antibody (AbCam) at a final concentration of 0.02 mg·mL^{-1}. F4/80 was detected with a rat monoclonal antibody (clone A3-1, AbD Serotec) diluted to 1:250. CD11c was detected with a hamster monoclonal antibody (clone N418, eBioscience) diluted to 1:250. ER-TR7 was detected with a rat monoclonal antibody (BMA Biomedicals) used at a final concentration of 0.01 mg·mL^{-1}. iNOS was detected with a rabbit anti-iNOS (BD Transduction Labs) used at 1 μg·mL^{-1}. Relmα was detected with a rabbit polyclonal antibody (Abcam) used at 0.8 μg·mL^{-1}. BrdU was detected with a rat monoclonal antibody (Abcam) used at 10 μg·mL^{-1}. Goat anti-Arg1 (Santa Cruz) and goat anti-Arg2 (Santa Cruz) were used at 2 μg·mL^{-1}. Rat anti-Gr1 mAb (clone RB6-8C5; kindly provided by L. D. Sibley, Washington University School of Medicine, St. Louis) was used at a 1:250 dilution. Rabbit anti-*Leishmania* arginase (kindly provided by B. Ullman, Oregon Health Sciences University, Portland, OR) was used at a 1:1,000 dilution. The following antisera were screened for reactivity to nitrotyrosine in IFN-γ/LPS-stimulated MΦs: rabbit anti-nitrotyrosine (Santa Cruz Biotechnology, sc-55256; Millipore, #06–284; Abcam, ab50185), mouse anti-nitrotyrosine (Santa Cruz Biotechnology, sc-32757), and rat anti-nitrotyrosine (Abcam, ab6479).

The following fluorescent secondary antibodies were used: Alexafluor555 goat anti-rabbit, Alexafluor633 goat anti-rabbit, Alexafluor488 goat anti-rat, Alexafluor555 goat anti-rat, Alexafluor633 goat anti-rat, Alexafluor568 goat anti-hamster, Alexafluor488 goat anti-chicken, Alexaflour555 donkey anti-goat, and Alexafluor647 donkey anti-rabbit (Invitrogen, all used at 2 μg·mL^{-1} concentrations).

Statement Identifying Institutional Committee Approving Animal Experiments. Animal handling and experiments were carried out in strict accordance with the recommendations in the *Guide for the Care and Use of Laboratory Animals* of the US National Institutes of Health (73). Animal studies were approved by the Animal Studies Committee at Washington University (protocol 20090086) in accordance with the Office of Laboratory Animal Welfare's guidelines and the Association for Assessment and Accreditation of Laboratory Animal Care International.

Mouse Infections. Female C57BL/6J mice (6–10 wk old; Jackson Labs) were injected s.c. in the left hind footpad with either 10^5 metacyclic WT or 10^6 metacyclic *lpg2*– parasites. Following infection with WT parasites, the mice developed lesions that resolved, as determined by the absence of footpad swelling relative to the uninfected foot, ~4 mo after infection. For the purposes of this study, persistent infections were defined as any time >1 mo following the resolution of footpad swelling. Unless otherwise indicated, studies with *lpg2*$^-$ were performed between 1 and 2 mo following infection. Possible *lpg2*$^-$ revertants showing amastigote virulence (74), defined here as

having >150 parasites in a single section, were excluded from analysis. PEMs were harvested and infected as described (75).

MΦ Infections. Starch-elicited PEMs were harvested and infected as described (75). Cells were activated with 100 U·mL^{-1} recombinant IFN-γ (Chemicon) and 100 ng·mL^{-1} LPS (Sigma) with or without the iNOS-inhibitor L-NIL (Cayman Chemical) at a concentration of 10 μM either immediately before or 72 h after infection. Nitrite production (determined by the Greiss assay; Sigma) and parasite survival were determined 24 h after MΦ stimulation. For these experiments, "percent survival" is defined as the ratio of the number of parasites per 100 MΦs compared with the same statistic in MΦs that were not treated with LPS/IFN-γ. For these experiments, percent survival is defined as the ratio of the number of parasites per 100 PEMs at either 24 or 96 h after infection versus the number of parasites per 100 PEMs 24 h earlier. To generate alternatively activated (M2) MΦs, PEMs were treated with media containing 100 U·mL^{-1} each of recombinant IL-4 (BD Pharmingen) and IL-13 (BD Pharmingen) for 48 h.

BrdU Staining and in Vitro Labeling Experiments. For all BrdU immunodetection experiments, paraformaldehyde-fixed samples were permeabilized with 0.1% Triton-X-100 in PBS for 15 min, washed in distilled water, and then immersed in 2 M HCl for 40 min to denature the DNA. After extensive washing with PBS, the samples were incubated in a blocking buffer containing PBS and 5% (vol/vol) normal goat sera and 0.1% (vol/vol) Triton-X-100 and were then stained as described in the text in the methods above. All BrdU stains used a 2-h incubation with the anti-BrdU antibody.

To test BrdU labeling in promastigotes in culture, either log- or stationary-phase *L. major* promastigotes were cultured in M199 media containing 0.1 mM BrdU (Sigma) for the indicated time, after which they were fixed in 4% (wt/vol) paraformaldehyde in PBS for 10 min and stained as described above. To test BrdU labeling in infected MΦs in vitro, PEMS were harvested and infected as described with stationary-phase parasites (75). Two hours after parasites were added, the MΦs were washed to remove extracellular parasites and placed in media containing 0.1 mM BrdU, where they were maintained. At 2 h, 1 d, 2 d, and 5 d postinfection, samples were fixed and stained as described above.

BrdU Incorporation Assay in Vivo. Several different methods were attempted to administer BrdU to the infected mice. In the preferred method, infected mice were injected every 3 h for 18 h with 200 μL of PBS containing 4 mg·mL^{-1} BrdU into the peritoneal cavity and 50 μL of this solution directly into the infected footpad, yielding a total dose of 6 mg BrdU. Mice were killed and frozen tissue sections prepared 24 h after the first dose of BrdU. In addition to our standard approach, we also tried administering BrdU in the drinking water (1 mg·mL^{-1}) via infusion using osmotic pumps (Alzet #2001D, 7.2 mg total dose) and single i.p. injections of 200 μL of PBS containing 4 mg·mL^{-1} BrdU. At 24 h after the first dose, the mice were euthanized and footpad tissue prepared and stained as described above. Volocity image analysis software (Improvision) was used to assist quantitation.

Tissue Preparation and Histological Staining. After euthanasia, infected draining popliteal lymph nodes or feet were harvested. The infected tissue was then fixed for 1 h at room temperature in 4% (wt/vol) paraformaldehyde in PBS. After fixation, tissues were incubated at 4 °C for 1 h in 10% and 20% (wt/vol) sucrose in PBS, followed by an overnight incubation in 30% sucrose. The tissues were then embedded in O.C.T. compound (Ted Pella, Inc.), cut into 10 μm-thick sections using a cryostat, and mounted onto microscope slides.

Unless otherwise indicated, tissue sections were stained as follows. Slides were washed in PBS, and tissues were then blocked and permeabilized in PBS containing 5% (vol/vol) normal goat sera (Vector laboratories) and 0.1% Triton-X-100 for 30 min. The sections were then stained with primary antibodies for 1 h. Unbound antibody was then washed off in PBS, and primary antibodies were detected with fluorescent secondary antibodies for 40 min, followed by a second wash in PBS. For some experiments, we needed to simultaneously stain tissue sections with different antibodies that were both generated in rabbits. To do this, the tissue was stained with an unlabeled rabbit primary antibody and a fluorescently labeled secondary antibody as described above. Next, the tissue was blocked for 30 min with a buffer containing 5% (vol/vol) normal rabbit sera (Sigma Aldrich), and then the second fluorescently conjugated primary antibody was used.

For TUNEL staining of the tissue sections, after all primary and secondary antibody staining was finished, the sections were stained with the In Situ Cell Death Detection Kit, TMR Red (Roche), according to the manufacturer's protocol. All sections were mounted in ProLong Gold reagent (Invitrogen).

Confocal Microscopy and Image Analysis. Microscopy was performed on a Zeiss 510 META confocal laser scanning microscope. Image analysis was performed using ImageJ or Volocity software.

Comparison of BrdU Staining Intensity. Samples were stained to detect parasite histones and BrdU, and three-dimensional confocal image stacks were acquired. Parasite nuclei were manually circumscribed in ImageJ software, and the average intensity in the anti-BrdU channel was determined from two-dimensional image stacks. As a control for comparison of iNOS staining intensity, PEMs were activated with media containing 100 U·mL^{-1} recombinant IFN-γ (Chemicon) and 100 ng·mL^{-1} LPS (Sigma). Twenty-four hours later, the cells were fixed in 4% (vol/vol) paraformaldehyde and stained in parallel with footpad tissue sections from PIP-infected mice with antibodies against *L. major* histones and iNOS, and nuclei were stained with TOPRO-3 (Invitrogen). To determine the fluorescence intensity of iNOS per cross-sectional area, the outline of each cell from a confocal stack was traced in Volocity software (Improvision), and the sum intensity of all "red" pixels (iNOS) in the selected area was divided by the total number of pixels in that area, yielding the mean pixel intensity for the cross-section.

Comparison of Arginase Staining Intensity Between Persistent Parasites and Promastigotes. Footpad tissue sections infected with persistent WT (PIPs) or log-phase WT promastigotes were labeled to detect parasite arginase with anti-*Leishmania* arginase antibody and parasite histones (with the fluorescently conjugated anti-histone antibody). Confocal images were acquired using identical settings, and then Volocity image analysis software was used to determine the total arginase fluorescence intensity on a per-cell basis. Confocal stacks were compressed into a single plane, and then the total arginase fluorescence intensity was determined within a 2.28-μm radius circle centered on parasite nuclei.

Statistics. Data are presented as the geometric mean ± SE. *P* values are calculated by the Student's *t* test method or ANOVA.

ACKNOWLEDGMENTS. We thank I.L.K. Wong for providing the antibodies against *L. major* histones, L. D. Sibley for providing the antibodies against F4/80 and CD11c, B. Ullman for providing the anti-*Leishmania* arginase antibody, and W. Beatty, C. Bogdan, D. E. Dobson, S. Khader, T. Margolis, D. Sacks, L. D. Sibley, T. Vickers, H. W. Virgin, and J. Uzonna, as well as the referees, for discussions and/or comments on the manuscript. This work was funded by NIH Grants R01 AI31078 and AI29646 (to S.M.B.) and a Berg/Morse Graduate Fellowship (to M.A.M.).

1. Monack DM, Mueller A, Falkow S (2004) Persistent bacterial infections: The interface of the pathogen and the host immune system. *Nat Rev Microbiol* 2(9):747–765.
2. Virgin HW, Wherry EJ, Ahmed R (2009) Redefining chronic viral infection. *Cell* 138(1): 30–50.
3. Pawlowski A, Jansson M, Sköld M, Rottenberg ME, Källenius G (2012) Tuberculosis and HIV co-infection. *PLoS Pathog* 8(2):e1002464.
4. Roizman B, Whitley RJ (2013) An inquiry into the molecular basis of HSV latency and reactivation. *Annu Rev Microbiol* 67:355–374.
5. Brown SP, Grenfell BT (2001) An unlikely partnership: Parasites, concomitant immunity and host defence. *Proc Biol Sci* 268(1485):2543–2549.
6. Singh OP, Hasker E, Sacks D, Boelaert M, Sundar S (2014) Asymptomatic *Leishmania* infection: A new challenge for *Leishmania* control. *Clin Infect Dis* 58(10): 1424–1429.
7. Pigott DM, et al. (2014) Global distribution maps of the leishmaniases. *eLife* 3:3.
8. WHO (2010) Control of the Leishmaniases: WHO Expert Committee on the Control of Leishmaniases. *World Health Organization Technical Reports* 949:1–186.
9. Bañuls AL, et al. (2011) Clinical pleiomorphism in human leishmaniases, with special mention of asymptomatic infection. *Clin Microbiol Infect* 17(10):1451–1461.
10. Wei XQ, et al. (1995) Altered immune responses in mice lacking inducible nitric oxide synthase. *Nature* 375(6530):408–411.
11. Stenger S, Donhauser N, Thüring H, Röllinghoff M, Bogdan C (1996) Reactivation of latent leishmaniasis by inhibition of inducible nitric oxide synthase. *J Exp Med* 183(4): 1501–1514.
12. Launois P, Louis JA, Milon G (1997) The fate and persistence of *Leishmania major* in mice of different genetic backgrounds: An example of exploitation of the immune system by intracellular parasites. *Parasitology* 115(Suppl):S25–S32.
13. Belkaid Y, et al. (2000) A natural model of *Leishmania major* infection reveals a prolonged "silent" phase of parasite amplification in the skin before the onset of lesion formation and immunity. *J Immunol* 165(2):969–977.
14. Okwor I, Uzonna J (2008) Persistent parasites and immunologic memory in cutaneous leishmaniasis: Implications for vaccine designs and vaccination strategies. *Immunol Res* 41(2):123–136.

15. Svobodová M, Votýpka J, Nicolas L, Volf P (2003) *Leishmania tropica* in the black rat (Rattus rattus): Persistence and transmission from asymptomatic host to sand fly vector *Phlebotomus sergenti*. *Microbes Infect* 5(5):361–364.
16. Kimblin N, et al. (2008) Quantification of the infectious dose of *Leishmania major* transmitted to the skin by single sand flies. *Proc Natl Acad Sci USA* 105(29): 10125–10130.
17. Aebischer T (1994) Recurrent cutaneous leishmaniasis: A role for persistent parasites? *Parasitol Today* 10(1):25–28.
18. Sacks DL (2014) Vaccines against tropical parasitic diseases: A persisting answer to a persisting problem. *Nat Immunol* 15(5):403–405.
19. Mandell MA, Beverley SM (2016) Concomitant immunity induced by persistent *Leishmania major* does not preclude secondary re-infection: Implications for genetic exchange, diversity and vaccination. *PLoS Negl Trop Dis* 10(6):e0004811.
20. Belkaid Y, Piccirillo CA, Mendez S, Shevach EM, Sacks DL (2002) CD4+CD25+ regulatory T cells control *Leishmania major* persistence and immunity. *Nature* 420(6915): 502–507.
21. Sacks D, Noben-Trauth N (2002) The immunology of susceptibility and resistance to *Leishmania major* in mice. *Nat Rev Immunol* 2(11):845–858.
22. Kaye P, Scott P (2011) Leishmaniasis: Complexity at the host-pathogen interface. *Nat Rev Microbiol* 9(8):604–615.
23. Belkaid Y, et al. (2001) The role of interleukin (IL)-10 in the persistence of *Leishmania major* in the skin after healing and the therapeutic potential of anti-IL-10 receptor antibody for sterile cure. *J Exp Med* 194(10):1497–1506.
24. Pagán AJ, et al. (2013) Tracking antigen-specific CD4+ T cells throughout the course of chronic *Leishmania major* infection in resistant mice. *Eur J Immunol* 43(2): 427–438.
25. Späth GF, et al. (2003) Persistence without pathology in phosphoglycan-deficient *Leishmania major*. *Science* 301(5637):1241–1243.
26. Bogdan C, et al. (2000) Fibroblasts as host cells in latent leishmaniosis. *J Exp Med* 191(12):2121–2130.
27. Uzonna JE, Späth GF, Beverley SM, Scott P (2004) Vaccination with phosphoglycan-deficient *Leishmania major* protects highly susceptible mice from virulent challenge without inducing a strong Th1 response. *J Immunol* 172(6):3793–3797.
28. Gratzner HG (1982) Monoclonal antibody to 5-bromo- and 5-iododeoxyuridine: A new reagent for detection of DNA replication. *Science* 218(4571):474–475.
29. Tattersall MHN, Brown B, Frei E, 3rd (1975) The reversal of methotrexate toxicity by thymidine with maintenance of antitumour effects. *Nature* 253(5488): 198–200.
30. Moll H, Flohé S, Röllinghoff M (1995) Dendritic cells in *Leishmania major*-immune mice harbor persistent parasites and mediate an antigen-specific T cell immune response. *Eur J Immunol* 25(3):693–699.
31. Gordon S (2003) Alternative activation of macrophages. *Nat Rev Immunol* 3(1):23–35.
32. De Trez C, et al. (2009) iNOS-producing inflammatory dendritic cells constitute the major infected cell type during the chronic *Leishmania major* infection phase of C57BL/6 resistant mice. *PLoS Pathog* 5(6):e1000494.
33. Goncalves R, Zhang X, Cohen H, Debrabant A, Mosser DM (2011) Platelet activation attracts a subpopulation of effector monocytes to sites of *Leishmania major* infection. *J Exp Med* 208(6):1253–1265.
34. Stenger S, Thüring H, Röllinghoff M, Bogdan C (1994) Tissue expression of inducible nitric oxide synthase is closely associated with resistance to *Leishmania major*. *J Exp Med* 180(3):783–793.
35. Prina E, Roux E, Mattei D, Milon G (2007) *Leishmania* DNA is rapidly degraded following parasite death: An analysis by microscopy and real-time PCR. *Microbes Infect* 9(11):1307–1315.
36. Liu B, Liu Y, Motyka SA, Agbo EE, Englund PT (2005) Fellowship of the rings: The replication of kinetoplast DNA. *Trends Parasitol* 21(8):363–369.
37. Carvalho LP, Pearce EJ, Scott P (2008) Functional dichotomy of dendritic cells following interaction with *Leishmania braziliensis*: Infected cells produce high levels of TNF-alpha, whereas bystander dendritic cells are activated to promote T cell responses. *J Immunol* 181(9):6473–6480.
38. Green SJ, Meltzer MS, Hibbs JB, Jr, Nacy CA (1990) Activated macrophages destroy intracellular *Leishmania major* amastigotes by an L-arginine-dependent killing mechanism. *J Immunol* 144(1):278–283.
39. Popovic PJ, Zeh HJ, 3rd, Ochoa JB (2007) Arginine and immunity. *J Nutr* 137(6, Suppl 2):1681S–1686S.
40. Bronte V, Serafini P, Mazzoni A, Segal DM, Zanovello P (2003) L-arginine metabolism in myeloid cells controls T-lymphocyte functions. *Trends Immunol* 24(6): 302–306.
41. Muleme HM, et al. (2009) Infection with arginase-deficient *Leishmania major* reveals a parasite number-dependent and cytokine-independent regulation of host cellular arginase activity and disease pathogenesis. *J Immunol* 183(12):8068–8076.
42. Müller AJ, et al. (2013) Photoconvertible pathogen labeling reveals nitric oxide control of *Leishmania major* infection *in vivo* via dampening of parasite metabolism. *Cell Host Microbe* 14(4):460–467.
43. Olekhnovitch R, Bousso P (2015) Induction, propagation, and activity of host nitric oxide: Lessons from *Leishmania* infection. *Trends Parasitol* 31(12):653–664.
44. Olekhnovitch R, Ryffel B, Müller AJ, Bousso P (2014) Collective nitric oxide production provides tissue-wide immunity during *Leishmania* infection. *J Clin Invest* 124(4): 1711–1722.
45. Liew FY, Millott S, Parkinson C, Palmer RM, Moncada S (1990) Macrophage killing of *Leishmania* parasite in vivo is mediated by nitric oxide from L-arginine. *J Immunol* 144(12):4794–4797.
46. Liu D, Uzonna JE (2012) The early interaction of *Leishmania* with macrophages and dendritic cells and its influence on the host immune response. *Front Cell Infect Microbiol* 2:83.
47. Kloehn J, Saunders EC, O'Callaghan S, Dagley MJ, McConville MJ (2015) Characterization of metabolically quiescent *Leishmania* parasites in murine lesions using heavy water labeling. *PLoS Pathog* 11(2):e1004683.
48. Cleary MD, Singh U, Blader IJ, Brewer JL, Boothroyd JC (2002) *Toxoplasma gondii* asexual development: Identification of developmentally regulated genes and distinct patterns of gene expression. *Eukaryot Cell* 1(3):329–340.
49. Betts JC, Lukey PT, Robb LC, McAdam RA, Duncan K (2002) Evaluation of a nutrient starvation model of *Mycobacterium tuberculosis* persistence by gene and protein expression profiling. *Mol Microbiol* 43(3):717–731.
50. Mirkovich AM, Galelli A, Allison AC, Modabber FZ (1986) Increased myelopoiesis during *Leishmania major* infection in mice: Generation of 'safe targets', a possible way to evade the effector immune mechanism. *Clin Exp Immunol* 64(1):1–7.
51. Pandit L, Kolodziejska KE, Zeng S, Eissa NT (2009) The physiologic aggresome mediates cellular inactivation of iNOS. *Proc Natl Acad Sci USA* 106(4):1211–1215.
52. Miller BH, et al. (2004) Mycobacteria inhibit nitric oxide synthase recruitment to phagosomes during macrophage infection. *Infect Immun* 72(5):2872–2878.
53. Blos M, et al. (2003) Organ-specific and stage-dependent control of *Leishmania major* infection by inducible nitric oxide synthase and phagocyte NADPH oxidase. *Eur J Immunol* 33(5):1224–1234.
54. Diefenbach A, et al. (1998) Type 1 interferon (IFNalpha/β) and type 2 nitric oxide synthase regulate the innate immune response to a protozoan parasite. *Immunity* 8(1):77–87.
55. Liu D, et al. (2009) *Leishmania major* phosphoglycans influence the host early immune response by modulating dendritic cell functions. *Infect Immun* 77(8):3272–3283.
56. Peters N, Sacks D (2006) Immune privilege in sites of chronic infection: *Leishmania* and regulatory T cells. *Immunol Rev* 213:159–179.
57. Courret N, et al. (1999) Presentation of the *Leishmania* antigen LACK by infected macrophages is dependent upon the virulence of the phagocytosed parasites. *Eur J Immunol* 29(3):762–773.
58. Reiner NE, Ng W, McMaster WR (1987) Parasite-accessory cell interactions in murine leishmaniasis. II. *Leishmania donovani* suppresses macrophage expression of class I and class II major histocompatibility complex gene products. *J Immunol* 138(6): 1926–1932.
59. Fruth U, Solioz N, Louis JA (1993) *Leishmania major* interferes with antigen presentation by infected macrophages. *J Immunol* 150(5):1857–1864.
60. van Lint AL, et al. (2005) Latent infection with herpes simplex virus is associated with ongoing CD8+ T-cell stimulation by parenchymal cells within sensory ganglia. *J Virol* 79(23):14843–14851.
61. Theil D, et al. (2003) Latent herpesvirus infection in human trigeminal ganglia causes chronic immune response. *Am J Pathol* 163(6):2179–2184.
62. Brandão GP, et al. (2011) Susceptibility to re-infection in C57BL/6 mice with recombinant strains of *Toxoplasma gondii*. *Exp Parasitol* 128(4):433–437.
63. Hiszczyńska-Sawicka E, Gatkowska JM, Grzybowski MM, Długońska H (2014) Veterinary vaccines against toxoplasmosis. *Parasitology* 141(11):1365–1378.
64. Centifanto-Fitzgerald YM, Varnell ED, Kaufman HE (1982) Initial herpes simplex virus type 1 infection prevents ganglionic superinfection by other strains. *Infect Immun* 35(3):1125–1132.
65. Gideon HP, Flynn JL (2011) Latent tuberculosis: What the host "sees"? *Immunol Res* 50(2-3):202–212.
66. Esmail H, Barry CE, 3rd, Young DB, Wilkinson RJ (2014) The ongoing challenge of latent tuberculosis. *Philos Trans R Soc Lond B Biol Sci* 369(1645):20130437.
67. Kapler GM, Coburn CM, Beverley SM (1990) Stable transfection of the human parasite *Leishmania major* delineates a 30-kilobase region sufficient for extrachromosomal replication and expression. *Mol Cell Biol* 10(3):1084–1094.
68. Vickers TJ, et al. (2006) Biochemical and genetic analysis of methylenetetrahydrofolate reductase in *Leishmania* metabolism and virulence. *J Biol Chem* 281(50): 38150–38158.
69. Reguera RM, Balaña-Fouce R, Showalter M, Hickerson S, Beverley SM (2009) *Leishmania major* lacking arginase (ARG) are auxotrophic for polyamines but retain infectivity to susceptible BALB/c mice. *Mol Biochem Parasitol* 165(1):48–56.
70. Späth GF, Beverley SM (2001) A lipophosphoglycan-independent method for isolation of infective *Leishmania* metacyclic promastigotes by density gradient centrifugation. *Exp Parasitol* 99(2):97–103.
71. Akopyants NS, et al. (2009) Demonstration of genetic exchange during cyclical development of *Leishmania* in the sand fly vector. *Science* 324(5924):265–268.
72. Anderson BA, et al. (2013) Kinetoplastid-specific histone variant functions are conserved in *Leishmania major*. *Mol Biochem Parasitol* 191(2):53–57.
73. Committee on Care and Use of Laboratory Animals (2011) *Guide for the Care and Use of Laboratory Animals* (National Academies Press, Washington, DC), 8th Ed.
74. Späth GF, Lye LF, Segawa H, Turco SJ, Beverley SM (2004) Identification of a compensatory mutant (*lpg2-REV*) of *Leishmania major* able to survive as amastigotes within macrophages without *LPG2*-dependent glycoconjugates and its significance to virulence and immunization strategies. *Infect Immun* 72(6):3622–3627.
75. Capul AA, Hickerson S, Barron T, Turco SJ, Beverley SM (2007) Comparisons of mutants lacking the Golgi UDP-galactose or GDP-mannose transporters establish that phosphoglycans are important for promastigote but not amastigote virulence in *Leishmania major*. *Infect Immun* 75(9):4629–4637.